Journal of Cosmology and Astroparticle Physics
An IOP and SISSA journal

Detectable neutrino fluxes due to enhanced cosmic ray densities in the Galactic Centre region

Julián Candia

The Abdus Salam International Centre for Theoretical Physics, Strada Costiera 11, 34014 Trieste, Italy
E-mail: jcandia@ictp.it

Received 12 May 2005
Accepted 19 October 2005
Published 2 November 2005

Online at stacks.iop.org/JCAP/2005/i=11/a=002
doi:10.1088/1475-7516/2005/11/002

Abstract. We examine in detail the detectability of a signal of diffuse high energy neutrinos produced in the Milky Way by the interaction of cosmic rays (CRs) with the interstellar medium (ISM). We show that highly inhomogeneous galactic CR densities arise naturally from large-scale drift effects and the inhomogeneous distribution of CR sources. In particular, the CR density in the Galactic Centre region (where the ISM density is maximal) could be an order of magnitude larger than the local CR density. Hence, the expected diffuse flux of neutrinos from the Galactic Centre region becomes enhanced and could be detected at energies above $\sim 10^4$ GeV in a km^3-size neutrino telescope within ten years of operation. The galactic anisotropy, which is the main signature of this flux, allows us to discriminate this signal from other possible extraterrestrial diffuse fluxes of high energy neutrinos.

Keywords: cosmic rays, ultra high energy photons and neutrinos, neutrino detectors, neutrino and gamma astronomy

ArXiv ePrint: astro-ph/0505346

JCAP11(2005)002

1475-7516/05/110002+17$30.00

Contents

1. Introduction

A new generation of neutrino telescopes is now opening an exciting new window on the high energy Universe. Indeed, planned or already built large neutrino detectors are capable of providing us with potentially revolutionary observations in the fields of particle physics, cosmology, astronomy and astrophysics.

Among different detection techniques proposed or already used, a particularly important role is played by under-ice and under-water optical Čerenkov detectors. This technique was very successfully implemented in the AMANDA detector [1] at the South Pole and in the Lake Baikal experiment [2]. The much larger, km^3-size detector IceCube [3] is currently under construction on the Antarctic ice, while other detectors (ANTARES, NEMO and NESTOR) are also being built in the Mediterranean Sea. While these under-ice/water optical Čerenkov detectors are sensitive at roughly TeV–PeV neutrino energies, which is essentially the range of interest in this work, other experiments extend the range of sensitivity up to ultra-high neutrino energies. Indeed, the radio Čerenkov detectors (such as RICE, ANITA, GLUE and SALSA) are sensitive roughly in the PeV–EeV energy range, while detectors making use of the Earth's atmosphere as a target volume (e.g. Fly's Eye, AGASA, HiRes and Auger) are sensitive at roughly EeV–ZeV energies.

Being able to escape even from very dense astrophysical environments, and to travel vast distances undeflected and unattenuated, neutrinos are a precious probe to the high energy Universe, which is complementary to both gamma-rays and cosmic rays. Pioneer work on high energy neutrinos produced in various astrophysical processes was accomplished roughly three decades ago (see e.g. [4]–[6]). Nowadays, a primary motivation for studying neutrinos above TeV energies is the identification of possible individual, point-like extragalactic sources such as active galactic nuclei (AGNs) and gamma-ray bursters (GRBs). It has also been proposed recently that jets accompanying core-collapse supernovae would produce detectable high energy neutrino bursts [7], which would reveal a connection between core-collapse supernovae and long duration GRBs. Furthermore, the existence of different kinds of neutrino sources located within the Galaxy has been suggested and studied (see [8] and references therein). However, the identification of point sources might be difficult to achieve, since they might be too weak to produce unambiguous directional signals in the detectors. Hence, also the detection of the corresponding

unresolved diffuse fluxes (i.e. the integrated fluxes produced by all sources) remains an important task. In order to achieve this goal, a sound knowledge of all other possible diffuse neutrino signals is obviously crucial.

At low energies, it is well known that *conventional* neutrinos produced by the decays of pions and kaons due to cosmic ray (CR) interactions in the atmosphere give the dominating signal [9, 10] (and this is, in fact, the only type of signal identified so far). At energies above a few hundred GeV, however, this component becomes strongly attenuated due to the fact that the parent mesons live longer and interact before decaying. The picture then looks more confusing, since different high energy neutrino fluxes of diverse origin, but possibly similar intensity, are expected to show up [11].

Besides the extragalactic fluxes mentioned above, other expected diffuse components of comparable (or even larger) intensity are, for instance, the so-called *prompt* fluxes arising from the decay of short-lived charmed particles produced by CR interactions in the atmosphere (see e.g. [12]–[14]). The evaluation of this prompt component requires taking into account next-to-leading-order processes in the charm production cross section, which is also dependent on the behaviour of the parton distribution functions at very low values ($x < 10^{-4}$) of the fraction of momentum carried by the partons, well below the range measured in present accelerators. The large uncertainties coming from the small-x extrapolation procedures are propagated on the estimated prompt neutrino fluxes and span more than an order of magnitude. A characteristic signature of this (roughly isotropic) signal is the flavour ratio $\nu_e{:}\nu_\mu{:}\nu_\tau \sim 1{:}1{:}\frac{1}{10}$, clearly different from the ratio 1:1:1 expected in a standard scenario for any extraterrestrial signal, due to the effects of neutrino flavour oscillations during propagation [15].

Another contribution to the high energy diffuse neutrino fluxes is that resulting from the interactions of the CRs present all over the Galaxy with the ambient gas in the interstellar medium (ISM) [5, 6], [16]–[18]. The very low densities in the ISM ($\rho_{\rm ISM} \simeq 1$ cm^{-3}) imply that essentially all mesons produced decay in this case without suffering any attenuation, and hence the neutrino fluxes are just the conventional ones from π, K and μ decays. Since these neutrino fluxes depend on the column density of the ISM along the particular direction considered, this component shows a significant anisotropy, being maximal in the direction to the Galactic Centre (GC) (and generally enhanced near the Galactic Plane), while being minimal in the direction orthogonal to it.

Although it was recognized that these diffuse fluxes of Galactic neutrinos could compete with the other expected contributions at high energies, a careful investigation of this signal was missing in the literature. Indeed, inhomogeneities in the CR density at different locations in the Galaxy were disregarded in previous investigations [6, 14], [16]–[19], in which variations in the ISM density were generally neglected as well. In contrast, in this work it is shown that large CR density inhomogeneities arise due to both large-scale drift effects and the inhomogeneous distribution of CR sources, producing an order-of-magnitude enhancement of the CR density in the GC region, where the ISM density is also maximal. Hence, this effect enhances the fluxes expected from the GC region for the diffuse signal of neutrinos produced in the Milky Way.

A detailed study of this contribution is important on its own, since its detection would imply the discovery of a new high energy neutrino signal, which would be also a new probe of cosmic rays and the interstellar medium. But, furthermore, it is also crucially important as a background in order to identify a real extragalactic flux, and hence a new probe of

JCAP11(2005)002

the high energy Universe. As already pointed out, measurements of the anisotropy in galactic coordinates could be used to distinguish between these different possibilities.

In the next section, we focus on the diffusion/drift scenario that describes the transport of CRs in the Galaxy under turbulent conditions [20]–[23]. While obtaining a sound agreement with local CR observations, we show that large inhomogeneities in the galactic CR density do arise as well. In section 3, we calculate the relevant neutrino fluxes and corresponding event rates, showing that the enhanced Galactic flux produced in the GC direction would dominate at high energies above $\sim 10^4$ GeV. Despite the small event rates, the detection of the diffuse Galactic signal in a km^3-size telescope such as IceCube is shown to be feasible and realistic. Finally, the conclusions are presented in section 4.

2. The transport of cosmic rays in the Galaxy

According to the standard picture, galactic CRs are accelerated in supernova remnants, the expanding shock wave fronts produced by the explosion of supernovae. This mechanism is suitable for producing high energy CR fluxes with power-law spectra. The different nuclear components generated in this way may have upper cutoffs at the energies $E_{cZ} \simeq ZE_c$, where E_c would correspond to the cutoff of the proton component. In the context of the supernova paradigm for the origin of galactic cosmic rays, this upper cutoff may range between $E_c \simeq 10^{15}$ and 10^{17} eV, depending on whether the strong shocks develop in the ISM or in the stellar wind of the predecessor star [24]. Higher cutoffs can be achieved, for instance, in a cooperative acceleration scenario, in which the collective effect of multiple stellar winds gives rise to an additional acceleration process [25]. For the sake of simplicity, here we assume a featureless production of galactic CRs (ignoring cutoffs) and study how the spectrum is shaped by the CR turbulent transport. Anyhow, the neutrino fluxes at energies above the PeV are too faint to be detectable (see the expected event rates in figure 5), and hence the high energy end of the galactic CR spectrum should not be relevant for the present discussion.

In order to characterize the transport of cosmic rays in the Galaxy, we will present here a simplified analytical realization of the diffusion/drift scenario [20]–[23]. It should be stressed that the previous investigations on this scenario were concerned only with the *local* observations of CRs, proposing suitable explanations of the CR spectrum and the observed knees, as well as of the composition and anisotropy measurements. Here we focus our attention instead on the *global* inhomogeneities of the CR population in the Galaxy arising from the inhomogeneous distribution of sources and from the onset of macroscopic large-scale drifts. Indeed, the main goal of this work is to show the relevant role played by these global inhomogeneities in the production of detectable neutrino fluxes from the GC region. In order to check the consistency and suitability of the approach used here, the model results for the local CR spectrum are required to agree with the corresponding experimental observations.

The region of propagation of the CR particles, the Galaxy, is often assumed for simplicity as a cylinder of radius R and height $2H$. For definiteness, here we will consider a flat model of the Galaxy with $R = 20$ kpc and $H = 2$ kpc. The galactic disc, which contains most of the visible matter, has a height of a few hundred pc and is embedded in a much larger structure, the galactic halo, which is thought to contain large amounts of dark matter. Associated to both the disc and the halo there are large-scale regular magnetic

JCAP11(2005)002

fields of a typical intensity of a few μG, which are oriented to a good approximation in the azimuthal direction. In the following, a single extended regular magnetic field $\mathbf{B_0}$ will be considered, without making any further distinction between disc and halo components.

The properties of this extended regular magnetic field are not well known, although observations seem to favour an antisymmetric structure (i.e. a field with opposite directions below and above the Galactic Plane), as would correspond to an A0 dynamo field configuration [26]. It is important to mention, however, that here we are adopting a simplified picture of the regular magnetic field. Indeed, while Zeeman splitting [27] and polarization observations at sub-millimetre wavelengths [28, 29] revealed very strong toroidal magnetic fields in the central molecular zone, other observations also indicated the presence of nonthermal radio filaments [30] and threads [31] in the Galactic Centre region, which appear to be directed nearly perpendicular to the Galactic Plane. Hence, the azimuthal symmetry assumed here should be regarded as a simplifying assumption that captures the global characteristics of the regular magnetic field in the Galaxy. The macroscopic drifts, anyhow, being large-scale currents that dominate the diffusion of cosmic rays at high energies, are not expected to be much dependent on the details of the magnetic field configurations.

Superimposed on the regular magnetic field, a random component associated to the turbulent interstellar plasma is known to exist, with a maximum scale of turbulence of order $L_{\rm max} \simeq 100$ pc. Since this random field component has a strength comparable to the field of the regular component, namely of the order of a μG, the transport of cosmic rays in the Galaxy takes place under highly turbulent conditions. Existing observational data [32] show that the spectrum of inhomogeneities may be the same for the density of the gas and for the magnetic field, and that it is close to a Kolmogorov spectrum. Hence, the random magnetic field can be assumed to be given by a power law spectrum with Fourier components giving rise to a magnetic energy density $\mathrm{d}E_{\rm r}/\mathrm{d}k \propto k^{-5/3}$, for $k \geq 2\pi/L_{\rm max}$.

A relativistic particle of charge Ze propagating across a regular field $\mathbf{B_0}$ describes a helical trajectory of radius $r_{\rm L} \sin\theta$, where $r_{\rm L}$ is the Larmor radius given by

$$r_{\rm L} = \frac{pc}{Ze|\mathbf{B_0}|} \simeq \left(\frac{E/Z}{10^6\ \mathrm{GeV}}\right)\ \left(\frac{\mu\mathrm{G}}{|\mathbf{B_0}|}\right)\ \mathrm{pc}, \tag{1}$$

while the pitch angle θ is the angle between the regular field and the particle velocity. In the presence of a superimposed random field component, the CRs scatter off the magnetic field irregularities with associated scales of order $r_{\rm L}$, changing their pitch angle but not their velocity. This collision mechanism, known as pitch angle scattering, provides an effective means of isotropization of the particle trajectories as long as the condition $r_{\rm L} \leq L_{\rm max}$ is met, which for instance corresponds to energies up to a few $\times 10^8$ GeV for protons propagating in the galactic magnetic fields. Another process known to contribute significantly to the diffusive transport of cosmic rays is the so-called field line random walk, which is the braiding and mixing of the magnetic field lines themselves [33]–[35].

Neglecting nuclear fragmentation and energy-loss processes such as ionization losses and adiabatic deceleration, the transport of high energy galactic cosmic rays is governed by diffusion. It should be remarked that adiabatic losses arising from convection in an expanding flow is an important mechanism in other contexts, for example in the escape of particles from expanding supernova remnants. However, in the absence of strong galactic

winds, this term can be safely neglected in the transport equations describing high energy CRs confined in the Galaxy. Thus, CR propagation takes place according to a diffusion equation,

$$\nabla \cdot \mathbf{J} = Q, \qquad \text{with } J_i = -D_{ij}\nabla_j \Phi, \tag{2}$$

where Q describes the distribution of sources, Φ is the CR differential flux and $\mathbf{J}$ the CR macroscopic current.

The diffusion tensor is given by

$$D_{ij} = \left(D_{\parallel} - D_{\perp}\right) b_i b_j + D_{\perp}\delta_{ij} + D_{\mathrm{A}}\epsilon_{ijk} b_k, \tag{3}$$

where $\mathbf{b} = \mathbf{B_0}/|\mathbf{B_0}|$ indicates the direction of the regular field, δ_{ij} is the Kronecker delta and ϵ_{ijk} the fully antisymmetric Levi-Civita tensor. The diagonal components of the diffusion tensor are $D_{\parallel}$ (which corresponds to the diffusion in the direction parallel to the regular magnetic field) and $D_{\perp}$ (associated to the diffusion along the transverse directions), which depend on short-scale turbulent fluctuations, while D_{A} is the antisymmetric (Hall) diffusion coefficient related to macroscopic drift effects.

Detailed numerical investigations of the behaviour of the different diffusion coefficients under highly turbulent conditions were recently performed [36]–[38]. Although the diffusion orthogonal to the regular magnetic field direction is typically much slower than the parallel one (unless the turbulence level is very high, since parallel and perpendicular motions then become similar), both $D_{\parallel}$ and $D_{\perp}$ have the same dependence on energy (as long as $r_{\mathrm{L}} < L_{\max}$, which is the case of interest for this work). Indeed, it is found that $D_{\parallel}, D_{\perp} \propto E^m$, where m characterizes the spectrum of the random magnetic field energy density, given by $\mathrm{d}E_{\mathrm{r}}/\mathrm{d}k \propto k^{m-2}$ [37]–[39]. In particular, $m = 1/3$ for the Kolmogorov case. Instead, the antisymmetric diffusion coefficient has a linear dependence on energy, $D_{\mathrm{A}} \propto E$ [20, 39]. As we will discuss further below, this stronger energy dependence of D_{A} plays a crucial role in the transport of high energy galactic CRs, since the knee ($E_{\mathrm{k}} \simeq 3 \times 10^6$ GeV) and the second knee ($E_{\mathrm{sk}} \simeq 4 \times 10^8$ GeV) of the spectrum can be explained as due to an enhancement in the escape of CRs while going from the transverse diffusion dominated regime (at low energies) to the Hall diffusion (drift) dominated regime (at high energies).

Besides the turbulent diffusion/drift scenario, many other models have been proposed in order to explain the CR observations around and beyond the knee region. For instance, it was recently proposed that most CRs at energies above ∼100 TeV could be originated in GRBs and that the knee feature could result from the transport of CRs produced by a recent nearby Galactic GRB [40]. Many other models for the origin of the knee are reviewed and compared in [41]. Anyhow, the diffusion/drift scenario is among the favoured models to explain the observations of galactic CRs [41]. It is based on very natural assumptions, it reproduces well the spectral shape and the composition observations, while it additionally predicts an anisotropy increase correlated with the knee of the spectrum [42], which is a particular feature that allows us to single out this scenario from all other proposals. Further evidence to clarify the origin of the CR knees will be available from mass group spectral observations and from more accurate measurements of the composition and the anisotropies, as expected for instance in the Kascade-GRANDE experiment [43].

JCAP11(2005)002

Since we are here assuming the cylindrical symmetry of the system and the regular field to be azimuthal, the parallel diffusion coefficient plays no role and the macroscopic current is simply given by

$$\mathbf{J} = -D_\perp \nabla\Phi + D_\mathrm{A}\mathbf{b}\times\nabla\Phi. \tag{4}$$

Here, D_A is considered to be a positive-definite quantity (corresponding to the diffusion of positively charged particles), while any sign changes arising from possible changes in the orientation of the regular field are contained in $\mathbf{b}$. This agrees with [21, 22, 38] but differs from the notation of [20].

In terms of cylindrical coordinates, equation (2) is explicitly given by

$$\left[-\frac{1}{r}\frac{\partial}{\partial r}\left(rD_\perp\frac{\partial}{\partial r}\right) - \frac{\partial}{\partial z}\left(D_\perp\frac{\partial}{\partial z}\right) + u_r\frac{\partial}{\partial r} + u_z\frac{\partial}{\partial z}\right]\Phi = Q, \tag{5}$$

where the drift velocities are

$$u_r = -\frac{\partial(D_\mathrm{A}b_\phi)}{\partial z} \tag{6}$$

and

$$u_z = \frac{1}{r}\frac{\partial(rD_\mathrm{A}b_\phi)}{\partial r}. \tag{7}$$

Notice that, since $b_\phi = \pm 1$, a change in the orientation of the regular field introduces a singular contribution to the drift velocities.

In order to deal with analytical solutions, we will consider here a simplified approach in which $D_\perp$ is spatially homogeneous, while $D_\mathrm{A} \propto r$ [20]. Let us consider a regular field antisymmetric with respect to the Galactic Plane (i.e. $b_\phi = \mathrm{sgn}(z)$). The drift velocities are

$$u_r = -2D_\mathrm{A}\delta(z), \qquad u_z = \frac{2D_\mathrm{A}}{r}\,\mathrm{sgn}(z), \tag{8}$$

i.e. the vertical drifts are directed outwards from the Galactic Plane, while on the plane there is a singular radial drift velocity directed towards the Galactic Centre.

Since the sources are located mainly in the Galactic Plane, their distribution is considered to be given by $Q = 2h_\mathrm{s}q(r)\delta(z)E^{-\beta}$, where $q(r)$ is the radial source distribution, h_s is a nominal vertical scale length and β the index of the source differential spectrum. As said above, we will consider that galactic CRs are accelerated in supernova remnants (SNRs). Hence, the source distribution will be given by the SNR radial profile [44]

$$q(r) = \left(\frac{r}{r_\odot}\right)^{\alpha_\mathrm{s}} \exp\left(-\beta_\mathrm{s}\,\frac{r-r_\odot}{r_\odot}\right) \qquad (\text{for } r \geq 3 \text{ kpc}), \tag{9}$$

with $\alpha_\mathrm{s} = 1.69$, $\beta_\mathrm{s} = 3.33$ and $r_\odot = 8.5$ kpc. Regarding the SNR population close to the GC (i.e. for $r < 3$ kpc), we will assume here a constant value (that matches the SNR population at $r = 3$ kpc), since a non-negligible SNR density is likely to exist in the GC region. This assumption is indeed consistent with the available observations [45].

As the Galaxy is assumed to be flat ($H \ll R$), one can neglect the radial gradients as compared to the gradients in z, and the solution to the diffusion equation is given by

$$\Phi^*(E;r,z) = E^{-\beta}\left(\frac{h_\mathrm{s}}{D_\mathrm{A}/r}\right)\left(\frac{1-\mathrm{e}^{-w(1-|z|/H)}}{1-\mathrm{e}^{-w}}\right)\int_1^{R/r}\mathrm{d}y\; q(yr)\; y^{-(1+2/(\mathrm{e}^w-1))}, \tag{10}$$

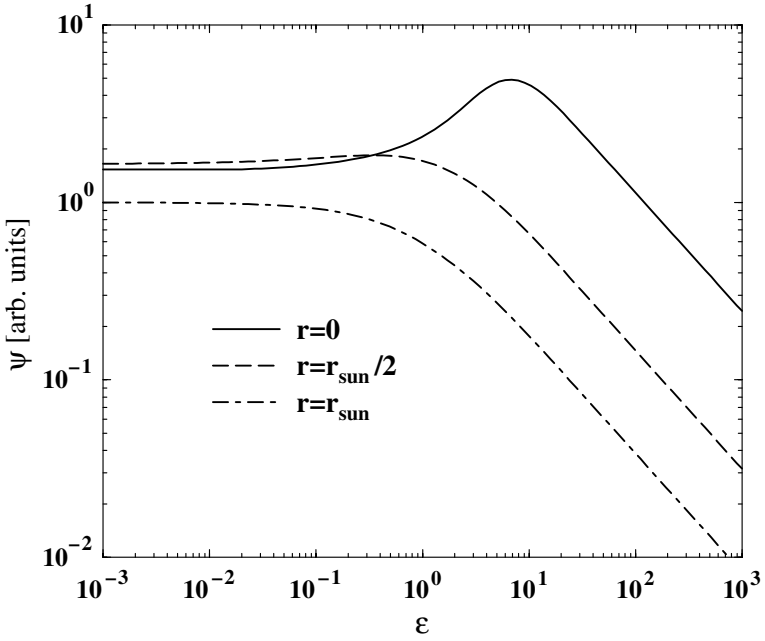

Figure 1. Single-component CR spectra for different locations on the Galactic Plane, as indicated, as functions of the adimensional, rigidity-scaled parameter $\epsilon = E/ZE_{\rm k}$ (where $E_{\rm k} = 3 \times 10^6$ GeV). The normalization is taken to be unity for the low energy local solution. Notice the large density enhancement produced in the Galactic Centre region by the onset of macroscopic drift effects.

where $w \equiv 2HD_{\rm A}/rD_{\perp}$ [20]. It should be noted that this flux, Φ^*, is a single-component solution (as if all CRs were, say, protons). Further below we consider the total CR flux, Φ, which takes into account all relevant nuclear contributions. Also notice that, as expected from the radial drift velocity pointing towards the GC, the density at a given radius r_0 receives the contribution from all sources located at larger radii, $r \geq r_0$, while the outwardly directed vertical drifts tend to remove the CRs from the Galactic Plane. In order to make explicit the dependence of w on the CR energy, we can conveniently rewrite it as

$$w = w_0 \left(\frac{E}{E_{\rm k}} \right)^{2/3}, \tag{11}$$

where $E_{\rm k} = 3 \times 10^6$ GeV is the energy of the knee and w_0 a constant parameter of order unity. To reproduce the local CR observations, we will assume here the plausible value $w_0 = 0.85$. As shown below (see figure 2), this choice allows us to obtain a sound agreement with experimental observations.

Figure 1 shows the single-component CR flux given by equation (10), for different locations $(r = 0, r_\odot/2, r_\odot)$ on the Galactic Plane $(z = 0)$, as a function of the adimensional, rigidity-scaled parameter $\epsilon = E/ZE_{\rm k}$. Notice that Φ^* was multiplied by a factor $E^{\beta+1/3}$ in order to produce flat solutions at low energies. Moreover, the normalization is taken to be unity for the low energy, local $(r = r_\odot)$ solution. For later convenience, this generic, single-component normalized solution with zero slope at low energies will be called $\psi(\epsilon)$.

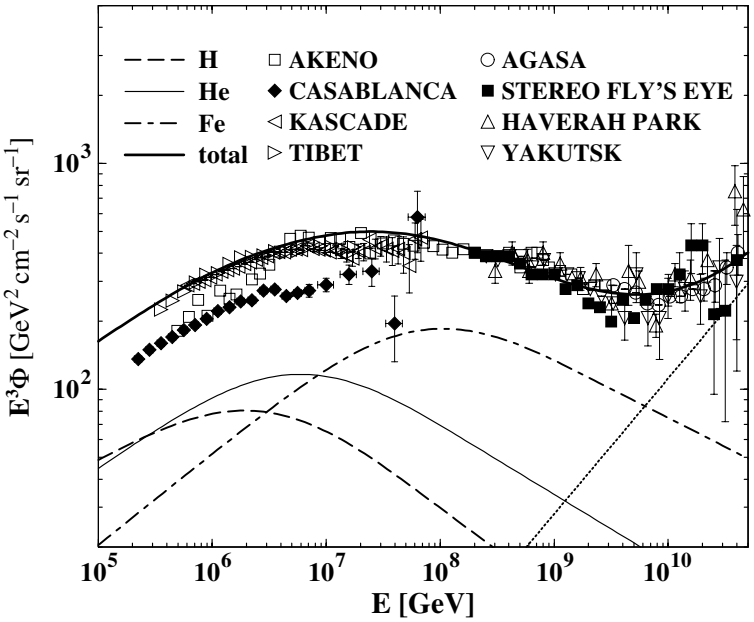

Figure 2. Local CR spectrum in the diffusion/drift scenario considered here, compared to experimental data sets. The main contributions to the total flux, which correspond to nuclei of H, He and Fe, are also indicated, as well as the assumed extragalactic flux, given by the dotted straight line.

As anticipated, the spectra show a change of slope $\Delta\alpha = 2/3$ driven by the $D_{\rm A}/D_{\perp}$ ratio. At low energies the CR transport is dominated by the transverse diffusion, $D_{\perp} \propto E^{1/3}$, while at larger energies the onset of drift effects enhances the escape as $D_{\rm A} \propto E$, hence producing a gradually steeper spectrum, which finally changes slope by $\Delta\alpha = 2/3$ in about a decade of energy. As will be shown further below, after summing over all CR nuclear components in the range $1 \leq Z \leq 28$ (appropriately scaling the results according to the magnetic rigidity E/Z) the envelope of the total spectrum nicely reproduces the observed knee (which results from the escape of the light component, mainly protons and He nuclei) as well as the second knee (which is due to the escape of the heavy component, i.e. the Fe-group nuclei). Another very interesting feature of the CR spectra shown in figure 1 is their significant spatial inhomogeneity, especially evident at high energies around and above the (local) knee. Indeed, in the high energy, drift dominated regime, the macroscopic CR currents are mainly driven by the large-scale regular magnetic fields. Hence, large accumulations (or depletions) of CRs at different locations in the Galaxy arise naturally by the same mechanism that is responsible for the CR first and second knees observed locally. This phenomenon, being a manifestation of large-scale CR propagation properties, is generally also dependent on the configuration of magnetic fields and the distribution of sources assumed.

In order to consider the contribution of all CR nuclear species from hydrogen ($Z = 1$) to nickel ($Z = 28$), we will assume that the spectra produced at the sources have constant (i.e. energy independent) spectral indices, which can then be inferred from low energy direct CR measurements. In the same vein, the relative contribution of different nuclear components can also be inferred from low energy observations. Hence, recalling the

Table 1. Cosmic ray fractional abundances (at the reference energy $E_0 = 10^3$ GeV) and spectral indices from hydrogen to nickel.

Z	f_Z	α_Z	Z	f_Z	α_Z	Z	f_Z	α_Z	Z	f_Z	α_Z
1	0.3775	2.71	8	0.0679	2.68	15	0.0012	2.69	22	0.0049	2.61
2	0.2469	2.64	9	0.0014	2.69	16	0.0099	2.55	23	0.0027	2.63
3	0.0090	2.54	10	0.0199	2.64	17	0.0013	2.68	24	0.0059	2.67
4	0.0020	2.75	11	0.0033	2.66	18	0.0036	2.64	25	0.0058	2.46
5	0.0039	2.95	12	0.0346	2.64	19	0.0023	2.65	26	0.0882	2.59
6	0.0458	2.66	13	0.0050	2.66	20	0.0064	2.70	27	0.0003	2.72
7	0.0102	2.72	14	0.0344	2.75	21	0.0013	2.64	28	0.0043	2.51

generic, locally normalized flux ψ defined above, the total CR flux is given by

$$\Phi(E) = \Phi_0 \sum_Z f_Z \left(\frac{E}{E_0}\right)^{-\alpha_Z} \psi\left(E/Z\right). \tag{12}$$

In this expression, $\Phi_0 = 3.5 \times 10^{-8}$ GeV^{-1} cm^{-2} s^{-1} sr^{-1} is the total CR flux at the reference energy E_0, hereafter adopted as $E_0 = 10^3$ GeV, f_Z are the fractional CR abundances at the same energy, and α_Z the low energy measured spectral indices, which were taken from the data compiled in [46, 47] (see table 1). Furthermore, we will assume an extragalactic isotropic proton component given by

$$\Phi_{XG} = 1.3 \times 10^{-28} \left(\frac{E}{10^{10}\ \text{GeV}}\right)^{-2.4} \text{GeV}^{-1}\ \text{cm}^{-2}\ \text{s}^{-1}\ \text{sr}^{-1}, \tag{13}$$

i.e. a flux similar to that considered in [14]. Notice that an extragalactic flux, if isotropic, permeates the Galaxy homogeneously, unless other processes different from diffusion (e.g. reacceleration) do occur.

Figure 2 shows the total local differential CR flux, along with its main components (protons, helium and iron), compared to data from several experiments. The extragalactic component is also shown separately. As can be observed clearly, a nice agreement between model results and experimental data is achieved even in this simplified analytical realization of the diffusion/drift scenario, and hence it provides a sound basis for the calculation of diffuse galactic neutrino fluxes.

3. The diffuse galactic neutrino flux

During their confinement in the Galaxy, CRs might interact with the ambient gas in the ISM, which is a very low density, non-relativistic plasma constituted mainly by atomic and molecular hydrogen. The mesons produced in these interactions decay before losing energy in secondary interactions, giving rise to neutrinos and photons. Moreover, the produced muons also decay without undergoing further energy losses and contribute to the neutrino signal as well.

The neutrino flux produced along a certain direction in the Galaxy is given by

$$\phi_\nu(E_\nu; b, l) = \int_{E_\nu}^{\infty} \mathrm{d}E\ \sigma_{\mathrm{pp}}^{\mathrm{inel}}(E)\ Y_\nu(E, E_\nu) \int_0^{x_{\max}} \mathrm{d}x\ \Phi_N(E, x)\ \rho_{\mathrm{ISM}}(x), \tag{14}$$

Table 2. Binned radial distribution of the ISM density, equation (16).

r (kpc)	0–0.3	0.3–0.6	0.6–2	2–4	4–6	6–8	8–12	12–20
n (cm^{-3})	38.1	2.23	1.91	1.04	1.14	0.87	0.40	0.18

where $\sigma_{\rm pp}^{\rm inel}$ is the inelastic proton–proton cross section, Y_ν is the neutrino yield (i.e. the mean differential neutrino spectrum produced in single proton–proton collisions), $\rho_{\rm ISM}$ the ISM nucleon number density, and $\Phi_N(E, x)$ the total (galactic plus extragalactic) nucleon CR flux at the galactic location denoted by x. Notice that the second integral involves the convolution of the CR flux with the ISM density along the line of sight defined by the galactic coordinates (b, l).

The total proton–proton cross section in terms of the centre of mass energy squared, s, is parameterized by

$$\sigma_{\rm pp} \simeq \left[35.49 + 0.307 \ln^2 \left(s/28.94 \text{ GeV}^2\right)\right] \text{ mb}, \tag{15}$$

which combines accelerator and very high energy CR data [48]. The inelastic cross section is given by $\sigma_{\rm pp}^{\rm inel} = K\sigma_{\rm pp}$, where $K = 0.8$ is the energy independent inelasticity used in this work.

As regards the ISM density distribution, a model consistent with the description given in [17] was assumed, namely

$$\rho_{\rm ISM}(r, z) = n(r) \exp(-z/0.5 \text{ kpc}), \tag{16}$$

where the binned radial profiles are given in table 2. It should be noticed that the ISM matter concentration peaks at the GC, i.e. in the same region where also the CR density is maximally enhanced.

In order to calculate the neutrino yield, Y_ν, we simulated fixed target proton–proton collisions by means of the PYTHIA 6.228 program [49], a general purpose high energy physics event generator. This program provides an accurate representation of event properties in a wide range of reactions, and particularly those involving strong interactions, where multihadronic final states are produced. Lacking an exact description, the program makes use of a combination of analytical results and various QCD-based models, which are then implemented to model hard subprocesses, initial- and final-state parton showers, remnants and underlying events, fragmentation and decays, etc. The decay of long-lived particles, which are considered to be stable in the context of collider physics applications, was enabled in our simulations in order to include the main galactic neutrino production channels.

Figure 3 shows the differential spectra of diffuse galactic neutrinos for different directions in the Galaxy. Here and throughout, fluxes are given per flavour, but adding neutrinos and antineutrinos. The interactions between CR particles and the ISM produce roughly twice as many ν_μ than ν_e, but at their arrival at the Earth the produced neutrinos are evenly distributed among the three flavours due to vacuum oscillations during propagation [15]. Since, as discussed above, both the ISM and the CR densities are largest in the GC region, the neutrino flux is maximally enhanced along the GC direction. Drift effects also enhance the galactic anisotropies, which are indeed the main signature to distinguish this diffuse galactic signal from other diffuse stationary extraterrestrial neutrino fluxes. Figure 3 also shows the neutrino flux that would be

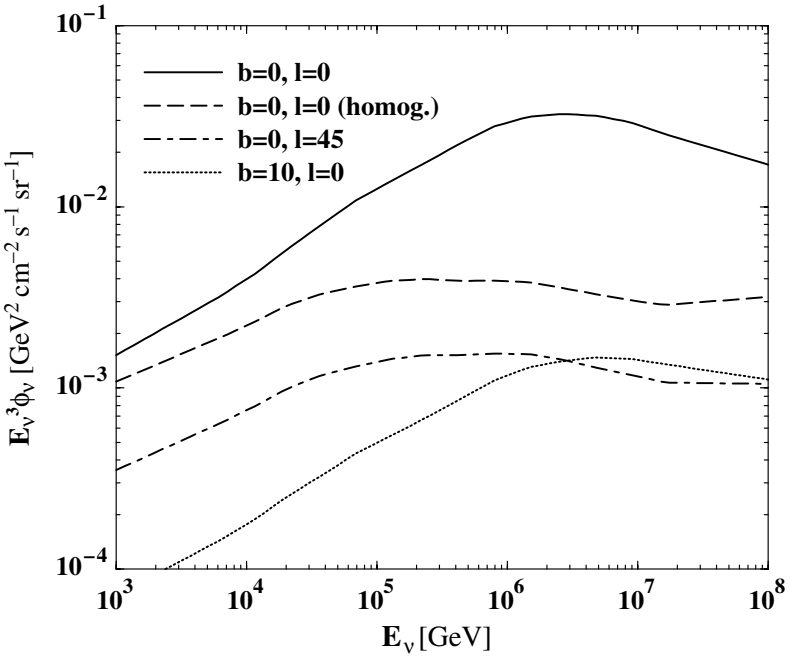

Figure 3. Differential spectra for diffuse Galactic neutrinos arriving at the Earth from different directions in the Milky Way. Galactic coordinates are given in degrees. Here and throughout, fluxes are given per flavour, but adding neutrinos and antineutrinos. Due to neutrino oscillations during propagation, the flavour ratio is ν_e:ν_μ:ν_τ = 1:1:1. For the sake of comparison, it is also shown the flux that would be produced from the GC direction if the CR density were homogeneous over the whole Galaxy (i.e. just taking into account the local CR observations).

produced in this same direction if the CR density were homogeneous over the whole Galaxy (i.e. ignoring the inhomogeneous distribution of CR sources and all propagation effects, and just taking into account the local CR observations). As anticipated, a large enhancement takes place at high neutrino energies above $\sim$ few $\times$ 10^4 GeV. Also notice the flux increment taking place at very high energies for the ($b = 10°, l = 0°$) direction, which is due to the vertical drifts that remove the CR particles from the Galactic Plane.

In order to compare the diffuse galactic signal to other high energy neutrino fluxes, figure 4 shows the galactic signal produced in the GC direction, together with the atmospheric conventional fluxes (averaged over zenith angle), the atmospheric prompt flux and the Waxman–Bahcall prediction for extragalactic neutrinos produced in GRBs [50]. Also shown is the latest AMANDA limit on the high energy neutrino flux, obtained from their shower analysis [1] and consistent with previous results from the BAIKAL experiment [2]. The two curves for the prompt atmospheric neutrino flux indicate the adopted range of small-x QCD uncertainties (for further details, see [19] and references therein). The prompt flux, however, could be larger than shown here, becoming indeed the dominating high energy signal for directions outside the GC region [19].

According to figure 4, the galactic flux from the GC is the dominant non-conventional high energy neutrino signal. As shown before, this signal is highly anisotropic in galactic

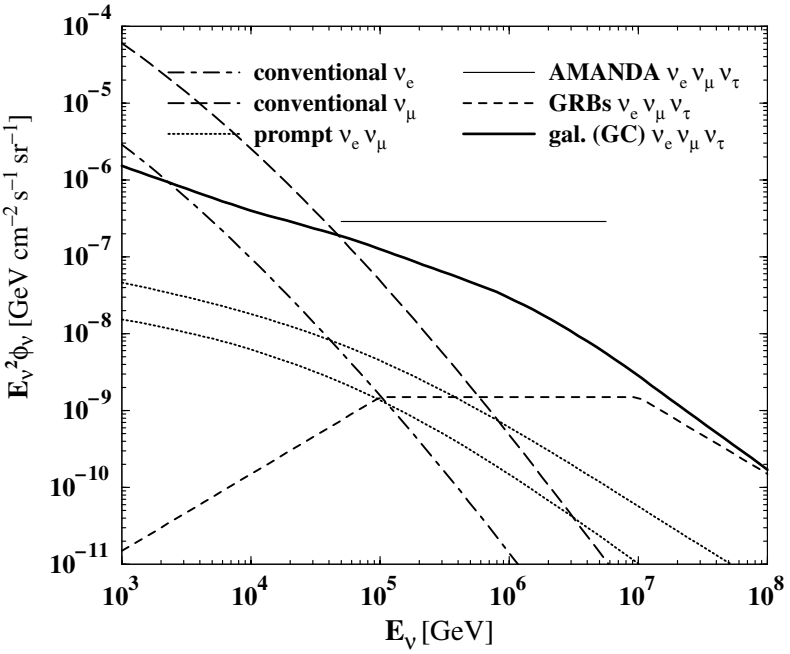

Figure 4. Diffuse galactic signal produced in the GC direction, compared to the conventional atmospheric fluxes (averaged in zenith angle), the prompt atmospheric flux and the Waxman–Bahcall prediction for extragalactic neutrinos produced in GRBs [50]. Also shown is the latest AMANDA limit on the high energy neutrino flux [1]. The two curves for the prompt atmospheric neutrino flux indicate the adopted range of small-x QCD uncertainties [19], although larger prompt fluxes are also possible.

coordinates (see figure 3) and the fluxes coming from outside the GC region are expected to fall by more than an order of magnitude. Hence, this scenario is optimistic as regards the detection of a high energy diffuse component of extragalactic origin. In this respect, very useful information on the galactic diffuse background (for directions outside the GC region) can be drawn from the detection of the galactic signal in the GC direction.

Figure 5 shows the integral event rates corresponding to the fluxes given in figure 4, as expected for a km^3-size detector observing the region ($|b| \leq 10°$, $|l| \leq 45°$) for ten years of data taking. We focus here on shower (cascade) event rates produced by downgoing neutrinos. Notice that the angular range considered is consistent with the $\sim$20° angular resolution expected for showers in IceCube. Being located at the South Pole, IceCube is capable of probing the GC region by means of downgoing neutrinos. For TeV energies, the downgoing ν_μ charged-current (CC) events are overcome by the much larger background of downgoing atmospheric muons. Instead, downgoing neutrinos can be measured by the observation of electromagnetic/hadronic cascades produced by neutrino interactions occurring within or near the detector fiducial volume [51, 52]. Furthermore, the observation of shower events (without lepton tracks) is particularly sensitive to the ν_e CC channel [19] and allows an effective reduction of the conventional background relative to any high energy signal (being either the prompt atmospheric flux, or an extraterrestrial

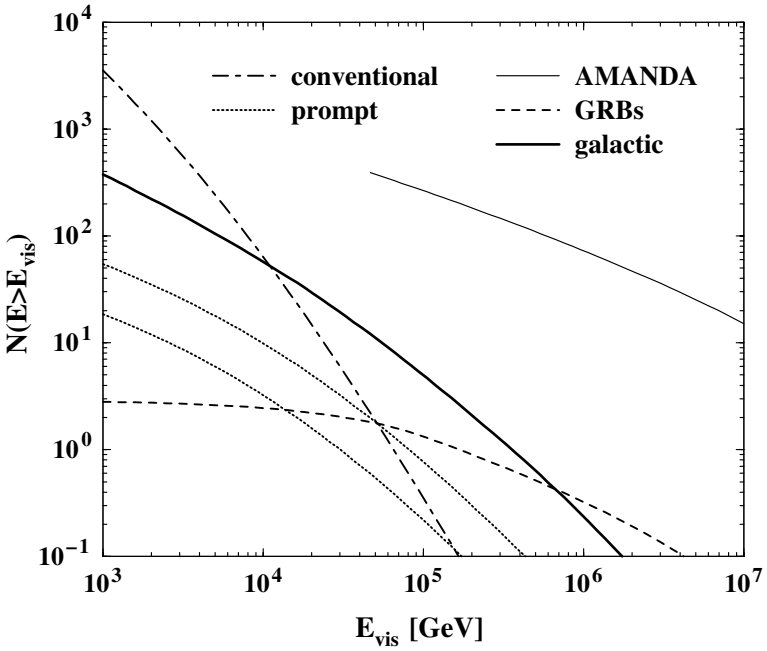

Figure 5. Integral shower event rates as a function of visible energy $E_{\rm vis}$, corresponding to the differential fluxes shown in figure 4. The rates are calculated for a km^3-size detector taking data from the region ($|b| \leq 10^\circ$, $|l| \leq 45^\circ$) for ten years. The line marked 'AMANDA' indicates the resulting integral spectrum assuming an E^{-2} power law, with no upper cutoff, normalized by the AMANDA differential limit [1] (which is actually given over a slightly smaller energy range).

component). In fact, the visible energy that can be reconstructed from a shower event, $E_{\rm vis}$, is roughly the same as the incoming neutrino energy for a CC ν_e interaction, while in a neutral-current (NC) interaction $E_{\rm vis}$ is smaller by a factor $\langle y \rangle \simeq 0.3$–$0.4$. This effect, convolved with the very steeply falling incoming spectra, and together with the additional suppression due to the smaller NC cross sections, yields NC ν_μ shower fluxes which are suppressed by roughly an order of magnitude relative to the shower fluxes arising via CC ν_e interactions. The shower detection channel was indeed recently proposed as a novel technique to isolate the prompt atmospheric flux (see [19]). A further analysis of the sensitivity of the shower channel in IceCube, as well as its comparison with the complementary upgoing and downgoing muon track channels, is accomplished in [52].

Despite the event rates being small, figure 5 shows that the detection of the diffuse galactic signal in a km^3-size telescope such as IceCube is feasible and realistic. A background subtraction of the conventional flux (which can be measured with large statistics at lower energies) would allow the identification of this relatively large galactic signal at energies above $\sim 10^4$ GeV.

Let us finally comment on the implications of this scenario for the observations of galactic diffuse gamma-rays above TeV energies, an exciting new window on the high energy Universe opened by the measurements by the CANGAROO, VERITAS, H.E.S.S. and Milagro Collaborations. Besides the hadronic (π^0 decay) channel, the galactic diffuse

photons can be produced by other processes such as high energy electron bremsstrahlung and inverse Compton scattering with the interstellar radiation field. Very recently, the Milagro Gamma Ray Observatory reported the first observations of a diffuse Galactic Plane gamma-ray signal at TeV energies [53].

Following a procedure analogous to that described at the beginning of this section, we calculated the photon differential flux produced by cosmic ray interactions in the ISM. In particular, the integral flux averaged over the region ($|b| \leq 5^\circ$, $40^\circ \leq l \leq 100^\circ$), i.e. the so-called Milagro Inner Galaxy, is given by $\phi_\gamma(E > 1\ \mathrm{TeV}) = 1.3 \times 10^{-10}\ \mathrm{cm}^{-2}\ \mathrm{s}^{-1}\ \mathrm{sr}^{-1}$, which is consistent with the Milagro results [53]. Further work on the implications of the drift-enhanced CR densities for the gamma-ray observations above TeV energies is under progress and will appear in a forthcoming paper.

4. Conclusions

The signal of diffuse neutrinos arising from interactions between CRs and the ISM in the Milky Way was reconsidered here taking into account a realistic scenario for the CR transport. The combined effect arising from an inhomogeneous distribution of CR sources (which, according to the standard picture, are assumed as SNRs) and from the onset of CR drifts (which could be also responsible for the observed knees in the local CR spectrum) is shown to produce large inhomogeneities in the galactic CR density. In particular, this phenomenon could drive a large accumulation of CRs in the GC region, where the ISM density is also largest, thus enhancing the fluxes expected for the diffuse galactic signal of neutrinos. From our estimates for the event rates expected in a large, km^3-size detector such as IceCube, the detection of this signal turns out to be quite plausible. These prospects of detection would be even better for larger experimental facilities, as for example in the proposed IceCube Plus project [54].

This neutrino flux would provide important information on the galactic CR puzzle and on related aspects of great astrophysical interest: the nature and the distribution of the CR sources, the structure and intensity of the galactic magnetic fields, the matter distribution of the ISM, etc. Furthermore, the detection of this extraterrestrial signal could be used to test for new physics beyond the standard model (see e.g. [55]–[57]).

The distinct signature that allows us to identify this diffuse galactic flux is the large galactic anisotropy. Indeed, the intensity from directions outside the GC region falls below the other expected high energy neutrino components. Hence, the detection of the galactic signal from the GC region could also provide very valuable information for understanding and estimating its impact as a background for measuring extragalactic neutrino fluxes in other directions.

Furthermore, an increased population of CRs in the GC region also could have an impact on the production of neutrons via proton–proton interactions [58] and nuclear photodisintegration due to ambient radiation fields [25, 59]. As pointed out in [25, 60], these neutron production and decay processes may lead to detectable gamma-ray and neutrino signals. Finally, let us recall that neutrons escaping from the GC region were also proposed as an explanation of the CR anisotropies observed by the AGASA and SUGAR experiments at EeV energies [58, 61]. However, these observations remain controversial, since they were not confirmed by the recent analysis performed with larger statistics by the Pierre Auger Collaboration [62].

Acknowledgments

The author is grateful to Simona Rolli for help with the numerical calculations of this paper, as well as for valuable discussions. John F Beacom, Esteban Roulet and Alexei Yu Smirnov are also acknowledged for their very helpful and encouraging remarks.

References

[1] Ackermann M *et al*, 2005 *Astropart. Phys.* **22** 339 [SPIRES]
[2] Aynutdinov V *et al* (BAIKAL Collaboration), 2003 *Proc. 28th Int. Cosmic Ray Conf. (Tsukuba)* p 1353
[3] Ahrens J *et al* (IceCube Collaboration), 2004 *Astropart. Phys.* **20** 507 [SPIRES]
[4] Berezinsky V S and Zatsepin G T, 1970 *Sov. J. Nucl. Phys.* **11** 111 [SPIRES]
[5] Berezinsky V S and Smirnov A Yu, 1975 *Ap. Space Sci.* **32** 461
[6] Stecker F W, 1979 *Astrophys. J.* **228** 919 [SPIRES]
[7] Ando S and Beacom J F, 2005 *Phys. Rev. Lett.* **95** 061103 [SPIRES]
[8] Bednarek W, Burgio G F and Montaruli T, 2005 *New Astron. Rev.* **49** 1
[9] Volkova L V, 1980 *Yad. Fiz.* **31** 1510 [SPIRES]
Volkova L V, 1980 *Sov. J. Nucl. Phys.* **31** 784 [SPIRES] (translation)
[10] Gaisser T K and Honda M, 2002 *Ann. Rev. Nucl. Part. Sci.* **52** 153 [SPIRES]
[11] Learned J G and Mannheim K, 2000 *Ann. Rev. Nucl. Part. Sci.* **50** 679 [SPIRES]
[12] Thunman M, Ingelman G and Gondolo P, 1996 *Astropart. Phys.* **5** 309 [SPIRES]
[13] Martin A D, Ryskin M G and Staśto A M, 2003 *Acta Phys. Polon.* B **34** 3273 [SPIRES]
[14] Candia J and Roulet E, 2003 *J. Cosmol. Astropart. Phys.* JCAP09(2003)005 [SPIRES]
[15] Athar H, Jezabek M and Yasuda O, 2000 *Phys. Rev.* D **62** 103007 [SPIRES]
[16] Domokos G, Elliott B and Kovesi-Domokos S, 1993 *J. Phys. G: Nucl. Part. Phys.* **19** 899 [SPIRES]
[17] Berezinsky V S, Gaisser T K, Halzen F and Stanev T, 1993 *Astropart. Phys.* **1** 281 [SPIRES]
[18] Ingelman G and Thunman M, 1996 *Preprint* hep-ph/9604286
[19] Beacom J F and Candia J, 2004 *J. Cosmol. Astropart. Phys.* JCAP11(2004)009 [SPIRES]
[20] Ptuskin V S *et al*, 1993 *Astron. Astrophys.* **268** 726 [SPIRES]
[21] Candia J, Roulet E and Epele L N, 2002 *J. High Energy Phys.* JHEP12(2002)033 [SPIRES]
[22] Candia J, Mollerach S and Roulet E, 2002 *J. High Energy Phys.* JHEP12(2002)032 [SPIRES]
[23] Candia J, Mollerach S and Roulet E, 2003 *J. Cosmol. Astropart. Phys.* JCAP05(2003)003 [SPIRES]
[24] Biermann P L, 1995 *Cosmic Winds and the Heliosphere* ed J R Jokipii *et al* (Tucson, AZ: University of Arizona Press)
[25] Anchordoqui L A *et al*, 2004 *Phys. Lett.* B **593** 42 [SPIRES]
[26] Han J L *et al*, 2002 *Radio Pulsars* (*APS Conf. Ser.*) ed M Bailes, D Nice and S Thorsett, at press [astro-ph/0211197]
[27] Yusef-Zadeh F *et al*, 1996 *Astrophys. J.* **466** L25 [SPIRES]
[28] Novak G *et al*, 2000 *Astrophys. J.* **529** 241 [SPIRES]
[29] Novak G *et al*, 2003 *Astrophys. J.* **583** L83 [SPIRES]
[30] Yusef-Zadeh F, Morris M and Chance D, 1984 *Nature* **310** 557 [SPIRES]
[31] Lang C C, Morris M and Echevarria L, 1999 *Astrophys. J.* **526** 727 [SPIRES]
[32] Armstrong J W, Cordes J M and Rickett B J, 1981 *Nature* **291** 561 [SPIRES]
[33] Jokipii J R, 1966 *Astrophys. J.* **146** 480 [SPIRES]
[34] Jokipii J R and Parker E N, 1969 *Astrophys. J.* **155** 777 [SPIRES]
[35] Forman M A, Jokipii J R and Owens A J, 1974 *Astrophys. J.* **192** 535 [SPIRES]
[36] Giacalone J and Jokipii J R, 1999 *Astrophys. J.* **520** 204 [SPIRES]
[37] Casse F, Lemoine M and Pelletier G, 2002 *Phys. Rev.* D **65** 023002 [SPIRES]
[38] Candia J and Roulet E, 2004 *J. Cosmol. Astropart. Phys.* JCAP10(2004)007 [SPIRES]
[39] Roulet E, 2004 *Int. J. Mod. Phys.* A **19** 1133 [SPIRES]
[40] Wick S D, Dermer C D and Atoyan A, 2004 *Astropart. Phys.* **21** 125 [SPIRES]
[41] Hörandel J, 2004 *Astropart. Phys.* **21** 241 [SPIRES]
[42] Antoni T *et al* (KASCADE Collaboration), 2004 *Astrophys. J.* **604** 687 [SPIRES]
[43] Navarra G *et al*, 2004 *Nucl. Instrum. Meth.* A **518** 207 [SPIRES]
[44] Case G and Bhattacharya D, 1996 *Astron. Astrophys. Suppl. Ser.* **120** 437
[45] Case G and Bhattacharya D, 1998 *Preprint* astro-ph/9807162
[46] Wiebel-Sooth B and Biermann P L, 1998 *Astron. Astrophys.* **330** 389 [SPIRES]

[47] Hörandel J R, 2003 *Astropart. Phys.* **19** 193 [SPIRES]
[48] Eidelman S *et al*, 2004 *Phys. Lett.* B **592** 1 [SPIRES]
[49] Sjöstrand T *et al*, 2001 *Comput. Phys. Commun.* **135** 238 [SPIRES]
[50] Waxman E and Bahcall J, 1999 *Phys. Rev.* D **59** 023002 [SPIRES]
[51] Kowalski M, 2003 *PhD Thesis* Humboldt-University, Berlin http://area51.berkeley.edu/manuscripts/
[52] Kowalski M, 2005 *J. Cosmol. Astropart. Phys.* JCAP05(2005)010 [SPIRES]
[53] Atkins R *et al*, 2005 *Preprint* astro-ph/0502303
[54] Halzen F and Hooper D, 2004 *J. Cosmol. Astropart. Phys.* JCAP01(2004)002 [SPIRES]
[55] Beacom J F *et al*, 2003 *Phys. Rev. Lett.* **90** 181301 [SPIRES]
[56] Beacom J F *et al*, 2004 *Phys. Rev. Lett.* **92** 011101 [SPIRES]
[57] Beacom J F *et al*, 2004 *Phys. Rev.* D **69** 017303 [SPIRES]
[58] Crocker R M *et al*, 2005 *Astrophys. J.* **622** 892 [SPIRES]
[59] Grasso D and Maccione L, 2005 *Astropart. Phys.* **24** 273 [SPIRES]
[60] Crocker R M, Melia F and Volkas R R, 2005 *Astrophys. J.* **622** L37 [SPIRES]
[61] Bossa M, Mollerach S and Roulet E, 2003 *J. Phys. G: Nucl. Part. Phys.* **29** 1409 [SPIRES]
[62] Letessier-Selvon A (for the Pierre Auger Collaboration), 2005 *Proc. 29th Int. Cosmic Ray Conf. (Pune, 2005)* [astro-ph/0507331]

JCAP11(2005)002